Relationship of Proton Release at the Extracellular Surface to Deprotonation of the Schiff Base in the Bacteriorhodopsin Photocycle

Yi Cao,* Leonid S. Brown,* Jun Sasaki,‡ Akio Maeda,‡ Richard Needleman,§ and Janos K. Lanyi*

*Department of Physiology and Biophysics, University of California, Irvine, California 92717 USA; ‡Department of Biophysics, Faculty of Science, Kyoto University, Kyoto 606-01, Japan; and §Department of Biochemistry, Wayne State University School of Medicine, Detroit, Michigan 48201 USA

ABSTRACT   The surface potential of purple membranes and the release of protons during the bacteriorhodopsin photocycle have been studied with the covalently linked pH indicator dye, fluorescein. The titration of acidic lipids appears to cause the surface potential to be pH-dependent and causes other deviations from ideal behavior. If these anomalies are neglected, the appearance of protons can be followed by measuring the absorption change of fluorescein bound to various residues at the extracellular surface. Contrary to widely held assumption, the activation enthalpies of kinetic components, deuterium isotope effects in the time constants, and the consequences of the D85E, F208R, and D212N mutations demonstrate a lack of direct correlation between proton transfer from the buried retinal Schiff base to D85 and proton release at the surface. Depending on conditions and residue replacements, the proton release can occur at any time between the protonation of D85 and the recovery of the initial state. We conclude that once D85 is protonated the proton release at the extracellular protein surface is essentially independent of the chromophore reactions that follow. This finding is consistent with the recently suggested version of the alternating access mechanism of bacteriorhodopsin, in which the change of the accessibility of the Schiff base is to and away from D85 rather than to and away from the extracellular membrane surface.

INTRODUCTION

During the light-driven reaction cycle ("photocycle") of the proton pump, bacteriorhodopsin (reviewed in Mathies et al., 1991; Rothschild, 1992; Oesterhelt et al., 1992; Lanyi, 1993), the connectivity of the protonated retinal Schiff base is first to the extracellular membrane side, and then it is changed to the cytoplasmic side. Because a protein conformation change ensures that the Schiff base proton is lost to one side before this *reprotonation switch* and regained afterward from the other (Kataoka et al., 1994), the transport mechanism is consistent with the long held alternating access hypothesis for ion pumps. It would be expected from the simplest version of such a model (Jardetzky, 1966; Wikström and Krab, 1979; Jencks, 1980; Tanford, 1983) that the release of the transported proton at the extracellular membrane surface and the uptake at the cytoplasmic surface alternate, i.e., occur at different times in the photocycle. Indeed, the release takes place before the uptake under most conditions, and at about the same time that a proton is transferred from the retinal Schiff base to D85 in the interior of the protein.

The proton release has been followed in single-turnover experiments after photoexcitation with a laser pulse, by measuring absorption changes of a pH indicator dye covalently bound to a surface residue, either to K129 (Heberle and Dencher, 1992; Heberle et al., 1993) or to cysteines introduced at various locations by site-specific mutagenesis (Scherrer et al., 1992; Alexiev et al., 1994b). Alternatively, the movement of the proton (and/or displacement of other charges) was determined from the photocurrent measured in oriented membranes (Keszthelyi and Ormos, 1989; Liu, 1990; Liu et al., 1990). The internal proton transfer, in turn, has been followed by measuring absorption changes of the chromophore in the visible, and of D85 in the infrared (Bousché et al., 1992; Souvignier and Gerwert, 1992). According to the results, D85 is not the origin of the released proton because this residue remains protonated until well after the proton is released. The nature of the proton release process at the surface and its relationship to the chromophore reactions are thus not yet understood, and the identity of the group XH (Braiman et al., 1988; Zimányi et al., 1992b; Balashov et al., 1993; Kono et al., 1993) that releases the proton to the aqueous phase, and how it is activated for the release, are still uncertain. This study will explore the correlation between the proton release, the protonation of D85, and the chromophore reactions that follow, and how it affects the alternating access hypothesis of the transport.

One of the problems in dissecting the reactions that lead up to deprotonation of the Schiff base is that there is a lack of consensus about the kinetic model that describes this part of the photocycle. The formation of deprotonated Schiff base (the M intermediate, measured at 410 nm) contains multiple (i.e., three or four) exponential components. At pH > 9, the complex formation kinetics for M is understood to originate from a change in the photocycle when an as yet unidentified

residue near the Schiff base is deprotonated in the unphotolyzed protein (Balashov et al., 1993; Kono et al., 1993). Near neutral pH, however, the origin of the multiphasic kinetics is controversial because it is not clear whether there is a heterogeneity in this pH region that affects the M formation. In one view, the rise components for M represent the differing photoreactions of a multiplicity of bacteriorhodopsin substates at the lower pH also (Hanamoto et al., 1984; Chronister et al., 1986; Diller and Stockburger, 1988; Eisfeld et al., 1993), and the observed rate constants of the kinetic components, therefore, correspond directly to the first-order rate constants of several independent $L \rightarrow M$ steps. In another view, there is no such heterogeneity, and the three kinetic components originate from a single reaction cycle containing two equilibration reactions after the photoexcitation followed by a step that is unidirectional at neutral pH, namely, $BR \xrightarrow{h\nu} K \leftrightarrow L$, $L \leftrightarrow M_1$, and $M_1 \rightarrow M_2$ (Zimányi et al., 1992b). Although in this case the observed rates are complex functions of the first-order microscopic rate constants, the three exponentials will correspond roughly to the equilibrations of K with L, and L with M_1, and to the M_1 to M_2 reaction. The first model is perhaps more intuitive, but recent results with proteins with double mutations, where large alterations in the M formation kinetics were well predicted from the changed rate constants in single mutants, favor the second model (Brown et al., 1994a). In the face of such complicated alternatives, however, some investigators have refrained altogether from interpreting the measured kinetics in terms of a model.

Until recently, the proton release at the extracellular surface was widely assumed to occur simultaneously with the deprotonation of the Schiff base, i.e., with the $L \rightarrow M$ reaction. Indeed, the activation enthalpies of one of the components of the formation of M and the proton release, as measured with a surface-bound dye, agreed with one another, suggesting that there is kinetic coupling between the two processes (Alexiev et al., 1994b). However, in another study (Heberle and Dencher, 1992) the activation enthalpy of the proton release was different than that of the two main M rise components, suggesting the contrary: that its rate is limited by a process other than the Schiff base to D85 proton transfer. It should be noted that the deprotonation of the Schiff base and the proton release are not always obligatorily linked to one another. At pH < 5 in the wild-type protein (Zimányi et al., 1992b), in the R82A, R82Q (Otto et al., 1990; Balashov et al., 1993; Cao et al., 1993a; Brown et al., 1994b), and in the D85E (Heberle et al., 1993) mutants, the proton release is strongly delayed relative to the rise of M. In the first three cases, the proton release occurs after M reached its maximum concentration and, in fact, well after the proton uptake at the cytoplasmic surface, resulting therefore in net proton *uptake* rather than net *release* in the cycle. This was confirmed by the direction of the pH change in the photostationary state. The fact that proton transport would take place under all of these conditions indicated that the vectoriality of these proton exchange reactions on the two membrane surfaces was preserved despite their lack of correlation with the chromophore

reactions. However, the photocurrent measured contained the same three time constants as the M formation, at least at pH > 8.5 (Liu, 1990). In that study, at lower pH only one M rise time constant was detected. The origins of this discrepancy with the dye experiments, and between the two reported dye measurements (Heberle and Dencher, 1992; Alexiev et al., 1994b), are not clear. They underscore the fact that the question of the correlation between proton release and chromophore reactions is still open.

Yet the release of the proton must be coupled, in some way, to the $L \rightarrow M$ chromophore reaction that precedes it. The subsequent events of the transport seem to be set off by the initial internal proton transfer that redistributes the proton between the Schiff base and D85. The drop in the pK_a of the proton release group XH, which may be R82 (Balashov et al., 1993), a water liganded to R82 (Braiman et al., 1988; Brown et al., 1993), or Y57 (Balashov et al., 1993; Kono et al., 1993), or a complex of these, to about 6 at this time in the photocycle (Zimányi et al., 1992b) must be related to abolition of the negative charge of D85. It was instructive to note that below pH 6 the first part of the photocycle is described by an $L \leftrightarrow M_1 \leftrightarrow M_2$ equilibrium, in which the concentration of L is greatly increased relative to higher pH (Zimányi et al., 1992b). Analysis of this phenomenon had indicated that it was the rate of the $M_2 \rightarrow M_1$ back-reaction that became greater at the lower pH, and this linked the proton release to the $M_1 \rightarrow M_2$ reaction rather than directly to the $L \rightarrow M_1$ reaction where D85 becomes protonated. Because the $M_1 \rightarrow M_2$ step had been associated with the change of the connectivity of the Schiff base from the extracellular to the cytoplasmic side (Váró and Lanyi, 1991a, b; Mathies et al., 1991) and, therefore, to the protein conformational change that occurs at this time in the photocycle (Koch et al., 1991; Nakasako et al., 1991; Subramaniam et al., 1993), this scheme raised the question whether the proton release is dependent on a previous protein conformation change, or vice versa.

Detection of the appearance of the proton at the surface with covalently bound dyes is an important part of the work aimed at understanding the causes of the proton release. Although pyranine detects protons in the bulk (Grzeisek and Dencher, 1986), most of the results are with fluorescein bound to the protein surface through reaction of its succinimidyl derivative with K129 (Heberle et al., 1993; Heberle and Dencher, 1990, 1992). However, some potential problems have been raised recently concerning what the dye detects at this position. The time constant of the protonation of fluorescein during the photocycle was found to be considerably changed when bound, as its iodoacetamido derivative, to cysteines introduced at various positions (e.g., along the loop that links helices D and E on the extracellular surface (Scherrer et al., 1992; Alexiev et al., 1994b)). Presumably, placing the dye at some positions oriented it better to be a direct proton acceptor without diversion to the surface water layer, whereas at others, in some cases a single residue away, the dye might be protonated from the aqueous phase after the release. Although the positions examined included K129 to which fluorescein was attached in the other kinetic studies,

direct comparisons were not possible. The M rise and the release of the proton are very significantly different in detergent-solubilized bacteriorhodopsin and in purple membranes, and the mutants containing cysteine were expressed in *Escherichia coli* and did not form a crystalline purple membrane lattice, whereas the K129 derivative was studied in the purple membrane form. Further, study of cysteine derivatives in combination with other mutations has shown that replacing a single charged residue on the surface significantly alters the surface potential (Alexiev et al., 1994a) and, therefore, might have affected proton release in the K129 derivative.

By expressing mutations in the homologous *Halobacterium salinarium* system, we produced purple membranes with fluorescein attached to single cysteines in recombinant bacteriorhodopsin. We report here studies on the surface properties of these purple membranes, and compare the chromophore reactions with proton release in this system. Furthermore, we used mutants in which the rate of formation of M and/or proton release are strongly altered to test further the $L \leftrightarrow M_1 \rightarrow M_2 + H^+$ model for proton release. The results provide some support of the model, but show also that the M kinetics and the proton release are not as simply related as this model would predict. This indicates that either the M_1 to M_2 reaction contains multiple, spectroscopically unresolved steps, or the proton release is the result of local residue interactions and occurs independently of other protein and chromophore changes. The alternating access hypothesis for transport for bacteriorhodopsin must take this into account. As suggested elsewhere (Kataoka et al., 1994), the alternating access cannot refer simply to the accessibility of the active site to the two membrane surfaces. Instead, access of the extracellular protein domain to the surface exists throughout the cycle, and the function of the reprotonation switch is to separate the Schiff base from this domain and connect it to the cytoplasmic domain.

MATERIALS AND METHODS

The site-specific residue replacements V130C, S35C, D85E, D85E/D96N, F208R, Y57F, Y57F/D96N, R82Q, and R82Q/D96N were introduced into the *bop* gene and expressed in *H. salinarium* with a vector based on a halobacterial plasmid, to be described elsewhere. We have reported on the D212N/D96N mutant previously (Cao et al., 1993b). The purple membranes containing these proteins were purified by a standard method (Oesterhelt and Stoeckenius, 1974).

Fluorescein was covalently linked to the single cysteines in V130C and S35C by reacting with iodoacetamidofluorescein, as described previously (Alexiev et al., 1994a). The wild-type protein bound virtually none of the dye. Covalent linkage to K129 was with fluorescein succinimidyl ester (Heberle and Dencher, 1992). The labeling stoichiometries were between 0.5 and 1 mol fluorescein/mol bacteriorhodopsin.

Static and time-resolved spectroscopy, and determination of proton release into the bulk with pyranine, were as described previously (Cao et al., 1993a, b). Unless otherwise stated, the experiments that measured proton release were done in 100 mM NaCl at pH 7.0, without buffer and with 20 mM bis-Tris propane. Because comparisons were made with earlier studies where 150 mM KCl and pH 7.5 was used (Heberle and Dencher, 1992; Heberle et al., 1993), we had ascertained that our results were not affected by these somewhat different conditions.

RESULTS

Surface potential and surface versus bulk pH

The properties of the two membrane surfaces were studied in two mutants in which V130 on the extracellular D-E interhelical loop or S35 on the cytoplasmic A-B interhelical loop was replaced with cysteine, and the pH indicator dye fluorescein was covalently attached to these residues. Fig. 1 shows spectroscopic titration of the V130C derivative. Fig. 1 A contains spectra of the dye (with the absorption of bacteriorhodopsin subtracted) at various bulk pH. As the pH is lowered, a major decrease of amplitude of the main band at 495 nm and a minor increase below 460 nm indicate titration of the OH group of fluorescein. At pH < 6 titration of the ring COOH decreases the amplitude at all wavelengths shown, but in the pH range of interest a good isosbestic point at 460 nm exists. Fig. 1 B shows the ratio of absorbance at the maximum and the isosbestic point as a function of pH, in the presence of 10 mM and 100 mM NaCl (*open* and *filled* symbols, respectively). The pK_a of free fluorescein is 6.7 (virtually independent of salt concentration between 10 and 100
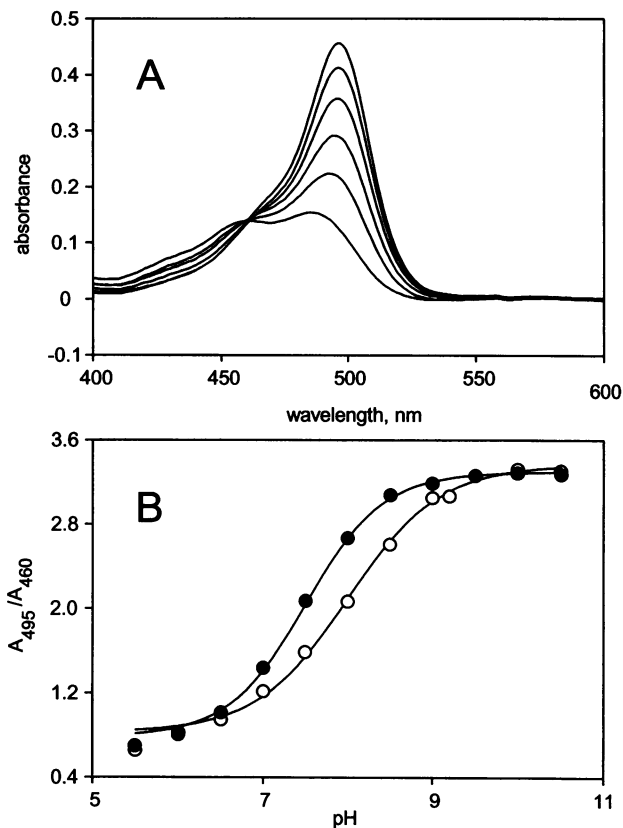

FIGURE 1 Spectroscopic titration of fluorescein covalently linked to the cysteine residue in V130C bacteriorhodopsin. (*A*) Spectrum of the covalently bound fluorescein, with the contribution of bacteriorhodopsin subtracted, at pH 9.5, 9.0, 8.5, 8.0, 7.5, and 6.5, in order of decreasing amplitude. Conditions: 10 μM bacteriorhodopsin, 5 mM NaCl, buffered with 2 mM aspartate, 2 mM succinic acid, 2 mM Bis-tris propane. (*B*) Absorbance amplitude ratio at 495 and 460 nm as a function of pH, with 10 mM NaCl (O) and 100 mM NaCl (●). Lines are the best fits of the Henderson-Hasselbalch equation, with the number of protons $n = 0.80$ for 10 mM and 0.95 for 100 mM salt.

mM, not shown). The curves in Fig. 1 B show that when the dye is attached to the bacteriorhodopsin surface the measured apparent pK_a is considerably higher and dependent on the salt concentration (8.0 and 7.5 at 10 and 100 mM NaCl, respectively). Furthermore, unlike the titration of the free dye, fitting the titration data to the Henderson-Hasselblach equation required that the order of the protonation reaction be less than 1 (cf. legend to Fig. 1).

The surface of bacteriorhodopsin contains an excess of negatively charged protein residues and a considerable amount of acidic lipids. The resulting negative surface charge and its measurements have been reviewed by Jonas et al. (1990). For the purposes of the calculation, the anomalous titration of the dye on the protein surface can be interpreted as reflecting a raised apparent pK_a (Alexiev et al., 1994a) or a lowered surface pH, caused by the negative surface potential. The two are equivalent. We have opted to treat the shift of the apparent pK_a as if it originated from a lowered surface pH relative to the bulk. The apparent surface pH as a function of bulk pH could be then calculated from the titration curves of free and bound fluorescein. The calculated ΔpH between surface and bulk from Fig. 1 B is then 1.7 and 1.2 at 10 and 100 mM NaCl, respectively. These values are in remarkably good agreement with the ΔpH predicted from fundamental assumptions for purple membranes (Szundi and Stoeckenius, 1989). Fig. 2 shows the surface versus bulk pH relationship for the fluorescein derivatives of V130C and S35C, in the presence of 10 and 100 mM NaCl. Data similar to those with V130C were obtained also with the fluorescein derivative of K129 (not shown). The solid lines are for zero surface potential (surface pH = bulk pH). At 100 mM NaCl the surface pH appears to be lower than the bulk pH, by about 1 unit on both extracellular and cytoplasmic surfaces. The ΔpH is nearly independent of the bulk pH in the range examined, particularly at the extracellular surface. This would be expected if the surface potential experienced by the dye were not dependent on pH. However, at 10 mM NaCl significant deviation from this simple relationship is evident at both surfaces. There are two problems. First, the calculated ΔpH between surface and bulk decreases with decreasing pH. The discrepancy is greater at the cytoplasmic surface. This is the same effect that produced a protonation stoichiometry less than 1 in Fig. 1 B, and implies that the surface potential is pH-dependent. The direction of the change is consistent with titration of surface groups with pK_a values between 7 and 8. A lower than first-order reaction in protons for the reprotonation of the Schiff base in the photocycle of D96N had been noted (Otto et al., 1989; Miller and Oesterhelt, 1990; Cao et al., 1991) and interpreted similarly (Miller and Oesterhelt, 1990). Partitioning of charged spin labels into the purple membranes had indicated, indeed, that the surface potential becomes more negative with increasing pH (Carmeli et al., 1980; Duñach et al., 1988). Second, the calculated surface pH values at 10 and 100 mM salt concentrations approach one another near pH 6, indicating the near absence of screening by the counterion layer. This should occur only at a pH where the surface potential is not
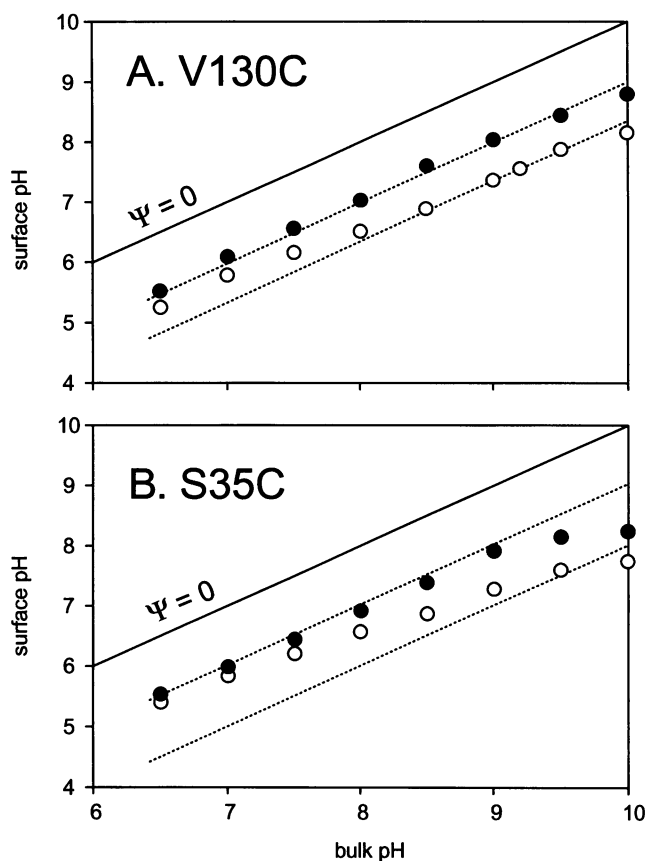

FIGURE 2 Dependence of calculated surface pH on bulk pH. (A) pH of the extracellular surface, from results with fluorescein bound to C130. (B) pH of the cytoplasmic surface, from results with fluorescein bound to C35. (○) 10 mM NaCl; (●) 100 mM NaCl. The solid line refers to zero surface potential, and the dashed lines are drawn arbitrarily to guide the eye.

significant, i.e., where the experimental lines intersect the zero potential line, but in Fig. 2 the calculated surface pH at this pH is still one pH unit lower than the bulk pH. A possible explanation would be that the distance between the fluorescein label and the protein surface is dependent on the pH, and at lower pH the dye detects a potential closer to the surface. This is a reasonable idea, because as fluorescein is titrated it becomes less charged at decreasing pH and could occupy a position closer to (and perhaps parallel with) the surface. Alternatively, the charges might be beneath the surface and, thus, incompletely shielded (cf. below).

The Boltzmann-Gouy-Chapman treatment of the effect of salt concentration on the surface potential (e.g., Jonas et al., 1990) predicts linear dependence of sinh $(e\Psi/kT)$ on $c^{-1/2}$, where $\Psi = 2.3kT/e(pH_{surface} - pH_{bulk})$ and c is the concentration of the monovalent salt. The slope of this line provides the surface charge density. Monomeric bacteriorhodopsin exhibited this predicted linear behavior, and the calculated charge densities at the two surfaces (labeled at residue 130 for the extracellular and at 160 for the cytoplasmic side) were close to what was expected (Alexiev et al., 1994a). We reproduced these results with monomeric V130C bacteriorhodopsin in Triton X-100 micelles (not shown). Fig. 3 shows
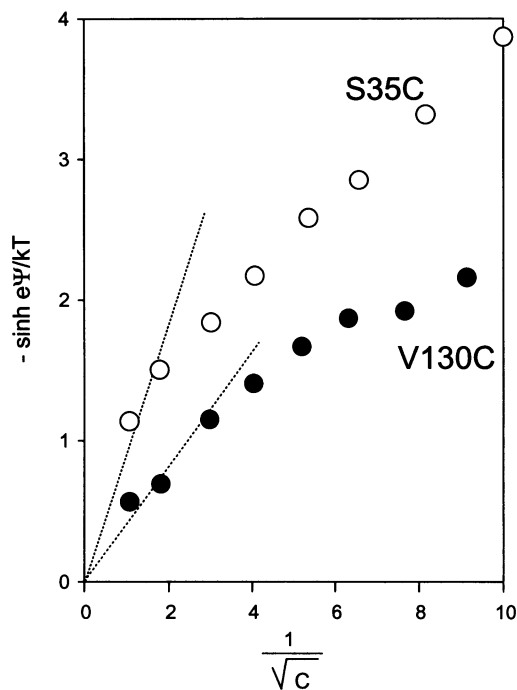
FIGURE 3   Gouy-Chapman plot of the dependence of surface potential on the concentration of NaCl. (O) Cytoplasmic surface, from results with fluorescein bound to C35; (●) extracellular surface, from results with fluorescein bound to C130. The lines are drawn arbitrarily to guide the eye.

results with V130C and S35C in purple membrane patches. The anomalies of the titration behavior in Fig. 2 recur in these experiments, indicating that it must be the presence of the lipids in the purple membrane that causes the deviation from ideal behavior. One interpretation of the data in Fig. 3 is that the curves deviate downward from linearity at low salt concentration, consistent with lower surface pH and, therefore, lowered surface potential, under these conditions (the lines are drawn arbitrarily, for guiding the eye). As in the case of the pH titrations (Fig. 2), the deviation from linearity is greater at the cytoplasmic surface. There is an excess of acidic lipids in the cytoplasmic half of the bilayer of purple membranes, but the number of charges and titrable groups is made uncertain and nonreproducible in different reports by partial methyl esterification of the lipids and tight binding of divalent cations (reviewed in Jonas et al., 1990). We could produce reasonable fits to the data in Figs. 2 and 3 by assuming 1–2 anionic surface groups with pK_a values below 6 and several titratable groups with pK_a values of 7 (not shown).

Another, or perhaps additional, interpretation of the deviation from linearity in Fig. 3 would be the presence of buried charges in purple membrane (but not in bacteriorhodopsin in detergent micelles), that cannot be shielded fully by cations. This would result in a non-zero intercept at the ordinate, which is also a possible explanation of the data points. Such a residual surface potential would explain also the observed lack of effect of salt at lower pH in Fig. 2 B, because the effect of such buried charges would begin to dominate once the surface charges are titrated.

It appears from the above that the surface pH, as detected by the indicator dye, is a rather complex and as yet unclear function of the bulk pH and the surface charges. Ideally, quantitating the proton released to the extracellular surface during the photocycle would require understanding this relationship. It is with the hope that, despite the complex behavior, nothing important will be lost if the surface pH is assumed to be a linear function of the number of protons released, that we describe the response of the dye during the photocycle in the section that follows.

Proton release kinetics in the wild-type protein

Indicator dyes covalently bound at the extracellular surface, e.g., to residues 129 or 130, detect the release of proton before its diffusion into the bulk (Heberle and Dencher, 1992). In monomeric bacteriorhodopsin, covalently bound fluorescein responds at least as fast as 20 μs to the released protons (Scherrer et al., 1992; Alexiev et al., 1994b). Thus, the dye should detect the appearance of protons fast enough on the surface of purple membranes, where the deprotonation of the Schiff base and the release of the proton are much slower than in the solubilized protein. Fig. 4 shows absorption changes at 410 nm (M kinetics) and net absorption changes at 495 nm from fluorescein, with changes after adding buffer subtracted (proton kinetics) in the V130C derivative as purple membranes. Fig. 4 A compares these changes at different temperatures, whereas Fig. 4 B contains results in H_2O and in D_2O at 20°C. The formation of M could be fitted satisfactorily to three exponentials at all temperatures between 5 and 35°C. Introduction of a fourth exponential yielded nonreproducible or widely scattered amplitudes and time constants. The decay of M was fitted with two exponentials. Although some of the dye traces appeared to be more complex than others, perhaps because of subtraction error (e.g., the 35°C trace in Fig. 4), the proton kinetics could be fitted in most cases with a single rise and a single decay exponential. The time constants and amplitudes of these fits at 20°C are given in Table 1. The effects of D_2O on the M formation agree with the magnitude of the isotope effect found earlier for M (Korenstein et al., 1976; Keszthelyi and Ormos, 1980), and for the time constant of the photocurrent associated with it (Keszthelyi and Ormos, 1980; Liu, 1990), for the component with the largest amplitude (the third component in our case). The effect of D_2O on proton release, as measured with a dye, has not been described previously. It is important to note that because the time constants in Table 1 refer to rates rather than the rate constants of the individual reactions, the observed slowing of the rates in D_2O cannot be interpreted directly in molecular terms. We use the deuterium isotope effect, instead, to establish correlation, or lack of correlation, between the kinetics of M and the proton release.

Superficially, in Table 1 the time constant of the proton release in H_2O appears to be associated with the third time constant of the formation of M. However, as reported previously (Heberle and Dencher, 1992), Fig. 5 A and Table 2 show that the activation enthalpy for the proton release is
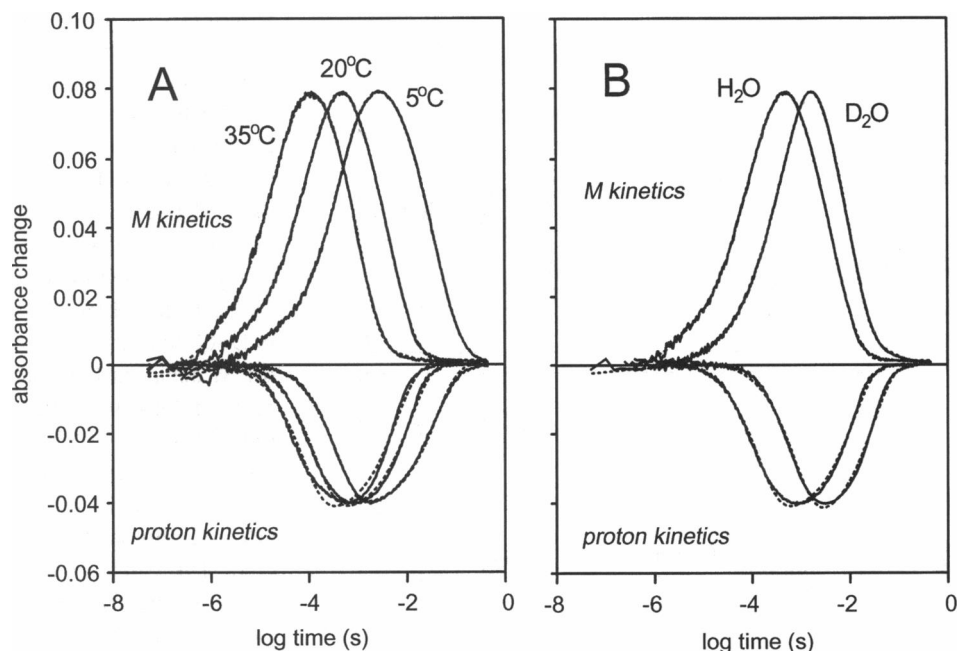
FIGURE 4 Kinetics of the M photointermediate and the fluorescein absorption changes after photoexcitation of V130C bacteriorhodopsin with fluorescein linked to C130. (——) Measured traces; (- - - -) fits of exponentials. (A) In H_2O, at 5, 20, or 35°C; (B) in H_2O or D_2O at 20°C.

TABLE 1 Kinetic parameters of the M photointermediate, and proton release and uptake, in wild-type and D85E bacteriorhodopsins, labeled with fluorescein at C130 or K129, respectively

| | Wild-type (fluorescein at C130) | | | | D85E (fluorescein at K129) | | | |
| | H_2O | | D_2O | | H_2O | | D_2O | |
	Amplitude	Time const.	Amplitude	Time const.	Amplitude	Time const.	Amplitude	Time const.
M-I	−0.11	1.7 μs	−0.04	5.8 μs	−0.37	0.6 μs	−0.41	4.0 μs
M-II	−0.25	35 μs	−0.17	101 μs	−0.49	6 μs	−0.40	18.7 μs
M-III	−0.64	144 μs	−0.79	670 μs	−0.14	131 μs	−0.19	152 μs
M-IV	0.93	4.7 ms	0.94	10 ms	0.51	2.7 ms	0.56	7.5 ms
M-V	0.07	46 ms	0.06	113 ms	0.49	13.2 ms	0.44	35 ms
H^+ release	1	134 μs	1	830 μs	0.76	164 μs	1	750 μs
H^+ uptake	−1	12 ms	−1	33 ms	−1	23 ms	−1	40 ms

Conditions: as in Figs. 4 and 6, 20°C. The components labeled M-I, M-II, and M-III are for M formation, and those labeled with M-IV, and M-V are for M decay.

well below (37 ± 2 kJ/mol) those of the M rise (47 ± 7, 73 ± 5, and 71 ± 4 kJ/mol for the three components, respectively). Furthermore, although the time constants of the third M rise and proton release agree fairly well at 20°C in H_2O, they are distinctly different in D_2O. Thus, the proton release cannot be linked *directly* to the deprotonation of the Schiff base or, indeed, to any process that limits the three processes reflected in the formation of M. Importantly, this conclusion does not depend on the fluorescein being bound to residue 130, as might have been suspected on the basis of differing time constants for the proton release with fluorescein at various positions on the D-E interhelical loop in monomeric bacteriorhodopsin. Virtually identical results are obtained when the dye is bound to residue 129 (Fig. 5B and Table 2).

Proton release kinetics in the D85E mutant

The overall rate of formation of M is greatly accelerated by the D85E residue replacement (Lanyi et al., 1992; Heberle

et al., 1993), but proton release is somewhat slowed (Heberle et al., 1993). These results would seem to suggest that the bulk of the additional methylene group in the glutamate changes the packing geometry near the Schiff base, E85, and the proton release group XH. Such a structural change should alter the barriers to the various reactions that take place in this region. We had found for other residue replacements that whenever a photocycle reaction was affected by a mutation, the activation enthalpy was always lowered (Brown et al., 1994b). Although that work was on reactions in the second half of the photocycle, the reported finding of essentially unchanged activation energy for the M rise components and for proton release in D85E relative to wild type (Heberle et al., 1993) seemed surprising. The experiments described for the wild-type protein in Figs. 4 and 5, therefore, were repeated with D85E with fluorescein covalently attached to K129.

Fig. 6 shows kinetics for M and protons in D85E, analogous to Fig. 4. As in Fig. 4, Fig. 6 A compares these changes
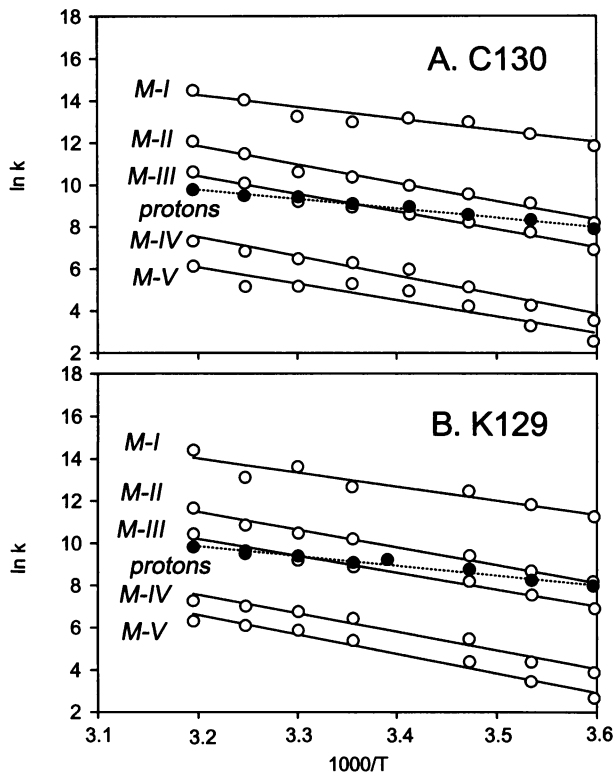
FIGURE 5 Arrhenius plot of the three formation (M-I, M-II, and M-III) and two decay (M-IV and M-V) components of the M photointermediate, and the release of protons (*protons*) in V130C bacteriorhodopsin with fluorescein bound to C130 (*A*), or wild-type bacteriorhodopsin with fluorescein bound to K129 (*B*). (O) M kinetics; (●) proton release.

TABLE 2 Activation enthalpies of the kinetic components of the formation and decay of the M photointermediate, and proton release, in wild-type and D85E bacteriorhodopsins labeled with fluorescein at C130 or K129

	Wild-type (fluorescein at K129)	Wild-type (fluorescein at C130)	D85E (fluorescein at K129)
M-I	55 ± 8	47 ± 7	47 ± 12
M-II	70 ± 3	73 ± 5	41 ± 7
M-III	66 ± 3	71 ± 4	26 ± 6
M-IV	73 ± 6	76 ± 7	88 ± 4
M-V	76 ± 7	65 ± 9	78 ± 6
H^+ release	38 ± 7	37 ± 2	21 ± 2

Enthalpies are in kJ/mol, calculated from Figs. 5 and 7. The components labeled M-I, M-II, and M-III are for M formation, and those labeled with M-IV and M-V are for M decay.

at different temperatures, whereas Fig. 6 *B* contains results in H_2O and in D_2O at 20°C. As for the wild type, the formation of M could be described with three exponentials, and its decay with two. Unlike in the wild type, proton release always exhibited a small second component (because of overlap readily evident only in the 5°C trace in Fig. 6*A*). The origin of this is very likely the heterogeneity of the D85E mutant: the two-thirds of the sample that contains protonated E85 at the pH tested and produces no M (Lanyi et al., 1992)

would release a proton, but on the cytoplasmic surface and in the millisecond time range, similar to D212N (Cao et al., 1993b) and D85N (Kataoka et al., 1994). As Fig. 7 and Table 2 indicate, the activation enthalpies for the second and third M formation components were considerably lower than in the wild type (41 ± 7 and 26 ± 6 kJ/mol for the second and third M rise components in D85E vs. 73 ± 5 and 71 ± 4 kJ/mol for the wild type), although they were nearly unchanged for the first M rise and the two M decay components (47 ± 12 for M rise; 88 ± 4 and 78 ± 6 kJ/mol for M decay in D85E vs. 47 ± 7 for M rise; 86 ± 10 and 89 ± 12 kJ/mol for M decay in the wild type). The activation enthalpy for proton release was likewise strongly lowered (21 ± 2 kJ/mol in D85E vs. 38 ± 5 kJ/mol in the wild type). We find, therefore, that consistent with many other bacteriorhodopsin mutations (Brown et al., 1994b), the activation enthalpies of the affected photocycle reactions are indeed significantly lowered. The cause of the difference from the previously reported results for D85E (Heberle and Dencher, 1992) is not clear, particularly because the activation enthalpies we find for M decay are in agreement with the earlier work. In D85E proton release nearly coincides with the slowest M rise component at all temperatures (Fig. 7), suggesting that, unlike in the wild type, proton release in this system is coupled to the third component of M formation. However, this conclusion is strongly contradicted by the results in D_2O, where the time constant for proton release is far greater than for any of the formation components of M (Table 1).

Delayed proton release in the F208R and D212N/D96N mutants

Fig. 8 shows M kinetics and proton release in two mutants in which the net charge of the extracellular protein domain is made more positive by either introducing an arginine residue or replacing an anionic aspartate. The deprotonation of the Schiff base (formation of M) is not greatly different from wild type in either mutant, but the subsequent proton release, detected here with pyranine, a pH indicator dye located in the bulk (Grzeisek and Dencher, 1986), is considerably delayed as in D85E (Fig. 6). The time constants for the release are 4.3 and 3.9 ms in F208R and D212N/D96N, respectively, i.e., well above the response time of pyranine to the appearance of protons in the bulk (0.5–1 ms in the wild type; Grzeisek and Dencher, 1986). The use of the double D212N/D96N mutant ensured that proton release from blue form of D212N, which does not produce M but releases protons from D96 on the cytoplasmic side (Cao et al., 1993b), will not occur. Fig. 8 shows that in these mutants the protons are released about 50 times slower than the deprotonation of the Schiff base. Significantly, the protons are released not while the Schiff base is still deprotonating as in wild type (Fig. 4) or D85E (Fig. 6), but at a time when it is already becoming reprotonated, i.e., its connectivity is already to D96 on the cytoplasmic side.

FIGURE 6 Kinetics of the M photointermediate and the fluorescein absorption changes after photoexcitation of D85E bacteriorhodopsin with fluorescein linked to K129. (——) Measured traces; (- - - -) fits of exponentials. (A) In H_2O, at 5, 20, or 30°C. (B) In H_2O or D_2O at 20°C.
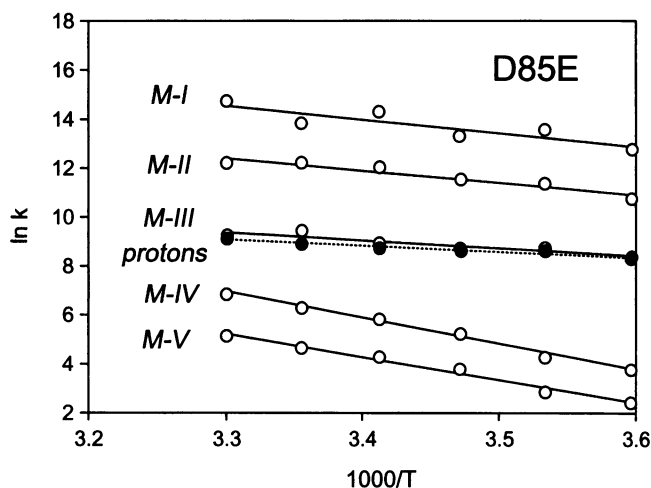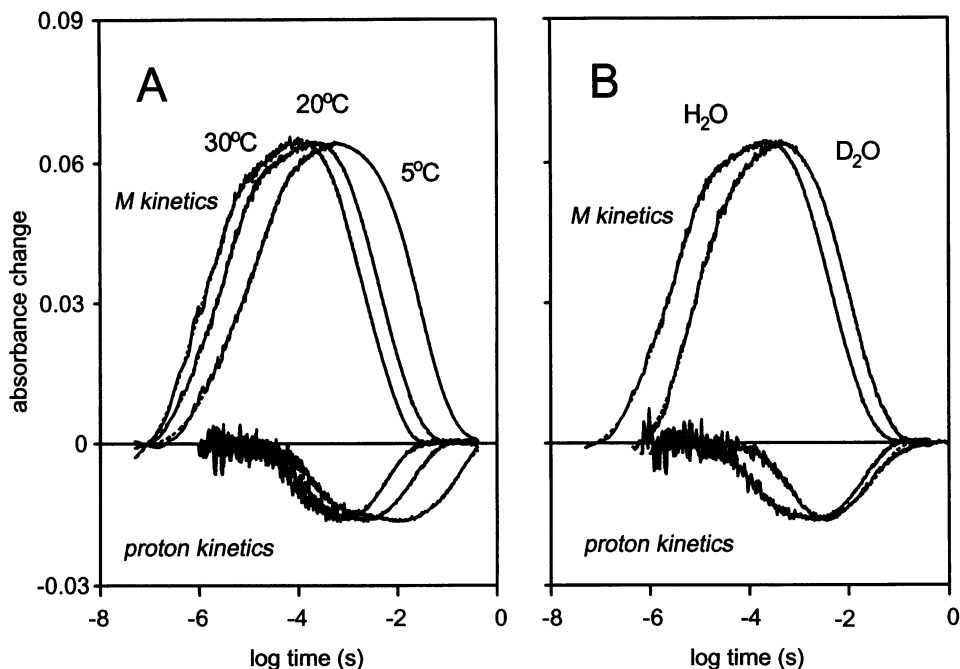

FIGURE 7 Arrhenius plot of the three formation (M-I, M-II, and M-III) and two decay (M-IV and M-V) components of the M photointermediate, and the release of protons (protons) in D85E bacteriorhodopsin with fluorescein bound to K129.

Identification of the third M rise component with the $M_1 \rightarrow M_2$ reaction

The more rapid formation of M than in wild type has been noted in D85E (Lanyi et al., 1992; Heberle et al., 1993) as well as in various other mutants. Closer analysis of the rise kinetics of M (Fig. 6, Table 1) now indicates that the main consequence of the D85E residue replacement is that the relative amplitudes of the three components are changed. In the wild type, the amplitude of the third component dominates and, therefore, the overall rise time is approximately the same as the time constant of the third component. In D85E,

the amplitudes of the first and, particularly, the second component dominate and, thus, the overall rise time assumes the faster time constants of these components. In view of this pattern of amplitudes and time constants, interpretation of the effect of the D85E mutation on the deprotonation of the Schiff base requires understanding the origin of the multiphasic M rise.

According to our analyses (Zimányi et al., 1992b), the photocycle reactions from the K state until the full formation of M are described approximately by the scheme $K \leftrightarrow L \leftrightarrow M_1 \rightarrow M_2$, where the K to L reaction is a relaxation of retinal bond torsions, the L to M_1 reaction is the equilibration of the proton between the Schiff base and D85, and at pH > 6 the M_1 to M_2 reaction includes proton release to the extracellular surface as well as the reorganization of proton-conductive pathways that allows the subsequent reprotonation of the Schiff base to be from D96. In this scheme, therefore, if the effect of the D85E residue replacement on M formation is a changed geometry for the proton donor and acceptor and, therefore, a change of their protonation equilibrium, it is the second M formation component that should be affected. This is largely the case.

This interpretation depends also on the third M rise component being, in fact, the decay of the L/M_1 equilibrium mixture to M_2 through the postulated $M_1 \rightarrow M_2$ reaction, which is unidirectional at pH > 7, as suggested. These two M substates were introduced originally for kinetic reasons (Váró and Lanyi, 1990), but when D96 was replaced with asparagine they could be distinguished also by their differing absorption maxima (Zimányi et al., 1992a). In the D96N mutant, M_1 absorbed at 411 nm, as both M substates in the wild type, but M_2 absorbed at 406 nm. This shift constitutes the basis for testing the suggested relationship of M rise kinetics and the
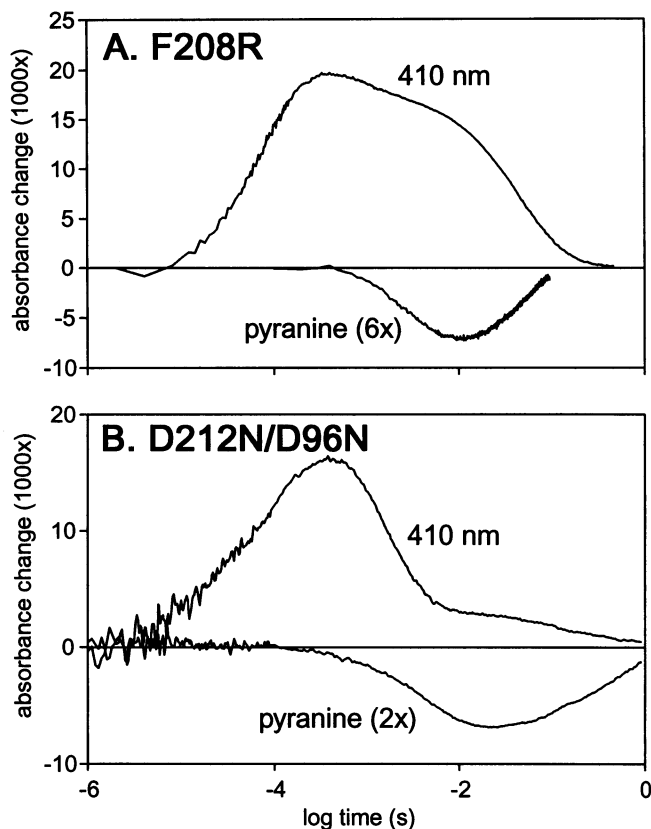
FIGURE 8 The kinetics of the M intermediate and the pyranine absorption changes that originate from proton release/uptake in the photocycles of (A) F208R and (B) D212N/D96N bacteriorhodopsins. The accumulation of M is followed by absorption change at 410 nm, the protons with the pH indicator dye, pyranine. Conditions for A: 2 M NaCl, pH 6.8, 50 μM pyranine, 22°C. Buffer was 10 mM phosphate *plus* 10 mM Bis-tris. For B the conditions were the same except the temperature was 25°C, and the buffer was 20 mM bis-Tris.

M substates. D96N is not ideal system for this because M_1 accumulates in large amounts only at pH $\geq$ 10 (Zimányi et al., 1992a). On the other hand, mutation of a number of residues in the extracellular region of the protein accelerates the formation of the M intermediate. Does the rapid rise of M in such mutants correspond to a greater $[M_1]:[L]$ ratio, i.e., to a lowered ΔpK_a between the Schiff base and the proton acceptor? We had determined the absorption maximum of M in A53G and A53G/D96N and found that the increased amplitude of M at earlier times corresponded to M_1, as expected from the scheme (Brown et al., 1994a). Here we report on R82Q in which the apparent time constant for the formation of M is about 1 μs at neutral pH (Thorgeirsson et al., 1991), as for R82A (Balashov et al., 1993), and on the corresponding R82Q/D96N double mutant. Fig. 9, A and B show difference spectra during the rise of the M state after photoexcitation (measured by optical multichannel spectroscopy), and Fig. 9, C and D show absorbance changes at 410 nm after photoexcitation (M kinetics, measured at a single wavelength) and the wavelength of the maximum of M, for R82Q/D96N and R82Q mutants, respectively. The maximum of the M state shifts to a shorter wavelength after the initial rise of M in the double mutant (Fig. 9, A and C), but not in the single mutant (Fig. 9, B and D). The shift to shorter wavelengths, therefore, is correlated with residue 96 not being an aspartate. We consider the initial unshifted absorption maximum of M as evidence that the M at this time consists of the M_1 substate, whereas the shifted maximum at later times reveals the M_2 substate. The results thus demonstrate that in the R82Q mutant the more rapid M formation reflects shift of the protonation equilibrium toward more complete transfer, as in A53G. Similar results were obtained with Y57F and Y57F/D96N (not shown), where the rise of M is also more rapid than in wild type.

FIGURE 9 M absorption maximum and kinetics, as determined by optical multichannel spectroscopy and from absorbance change at 410 nm after photoexcitation, in R82Q/D96N (A and C) and R82Q (B and D). (A and B) Difference spectra at 3.8, 8.4, 38.6, 80.2, 360, and 1.6 ms (the last time point is not shown in A). (C and D) Traces represent absorbance, the circles the wavelengths of the maxima. The latter were determined by fitting Gaussian curves to the 390–420 nm region of time-resolved difference spectra in A and B. For the comparison, the amplitude of the trace in D was normalized to that in C. Conditions: 2 M NaCl, 10 mM phosphate *plus* 10 mM Bis-tris propane, pH 6.8, 15 μM bacteriorhodopsin.
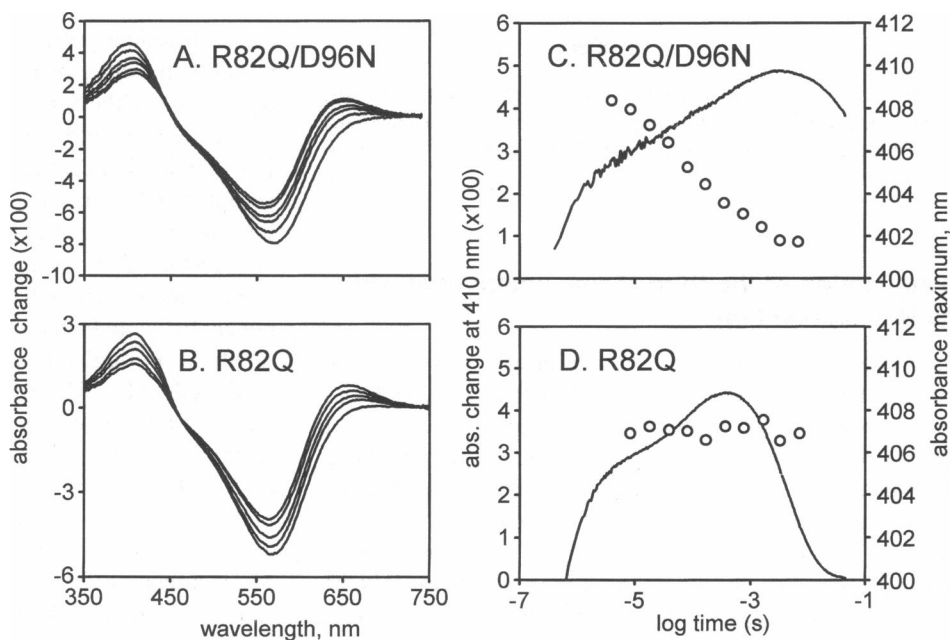
Fig. 10 shows the results from the same experiment, but with D85E and D85E/D96N. The difference spectra in Fig. 10, *A* and *B* are more complex than in Fig. 9, because at neutral pH E85 is partially protonated and the sample is a mixture of a red form that produces M upon photoexcitation and a blue form that produces intermediates other than M (Lanyi et al., 1992). Nevertheless, it is evident from the shift in the maximum of M in the double mutant that, as in R82Q, M_2 is produced approximately together with the last phase of M formation.

DISCUSSION

One of the most intriguing questions in the bacteriorhodopsin photocycle is how (and whether) the steps in the reaction sequence are causally linked to the preceding ones. For example, we had found that the loss of proton from D96 that normally reprotonates the Schiff base in the M→N reaction does not depend on previous deprotonation of the Schiff base (Cao et al., 1993b). In the present study, we explored the relationship of proton release to deprotonation of the Schiff base and the ensuing reactions of the photocycle to define the details of the alternating access hypothesis as applied to proton transport by bacteriorhodopsin (Kataoka et al., 1994). However, describing the kinetics is particularly difficult for the reactions in the extracellular domain, where the structure of the protein is not well understood and the interactions of various functional residues are multiple and complex (Humphrey et al., 1994; Sampogna and Honig, 1994). Although the proton release at the extracellular membrane surface is certainly triggered by the internal proton transfer from the Schiff base to D85, it is not obvious whether the connection between the two processes is direct. One would expect that the mechanism of proton release would be based on

the changing interaction of D85 with the proton release group XH upon its protonation (Balashov et al., 1993), and the consequently lowered pK_a and perhaps spatial disposition of XH relative to the protein-water interphase. If so, proton release to the extracellular surface will depend on interactions that do not necessarily involve the Schiff base, and the access of D85 will be distinct from the access of the Schiff base.

Fluorescein covalently bound to the extracellular protein surface appears to respond to changes in surface pH as expected, although when the pH is lower than 8, or the pH changes are large, titration of surface lipid groups and perhaps other influences will cause deviation from Gouy-Chapman behavior (Figs. 2 and 3). For very accurate measurements of proton kinetics, these anomalies will be a problem. For the purposes of this study, we assumed, however, that the kinetics of proton release can be measured accurately enough with the absorbance changes of this dye. The pH dependence of the kinetics of L and M had demonstrated earlier that as the pH was lowered to 6 an $M_2 \rightarrow M_1$ back-reaction appeared concurrently with a decrease of the proton release (Zimányi et al., 1992b). This was attributed to the pH being near the pK_a of the proton release group XH. Release of the proton above this pK_a, as measured with pyranine located in the bulk in that work, thus contributed to the unidirectionality of the $M_1 \rightarrow M_2$ and, therefore, of the preceding $L \rightarrow M_1$ reaction. In molecular terms, this would mean that D85 reversibly lowers the pK_a of XH, perhaps by its reorientation toward XH when protonated by the Schiff base, and it is only once XH is dissociated that the protonation equilibrium between the Schiff base and D85 shifts overwhelmingly toward protonation of D85. This interpretation is strengthened by the results with fluorescein, which on the one hand demonstrate parallel changes in M formation kinetics and proton release upon replacement of D85 (Fig. 7,

FIGURE 10 M absorption maximum and kinetics, as determined by optical multichannel spectroscopy and from absorbance change at 410 nm after photoexcitation, in D85E/D96N (*A* and *C*) and D85E (*B* and *D*). (*A*) Difference spectra at 6, 15, 40, 100, 250, and 0.6 ms. (*B*) Difference spectra at 6, 10, 15, 100, and 0.6 ms. (*C* and *D*) Traces represent absorbance, the circles the wavelengths of the maxima. The latter were determined by fitting Gaussian curves to the 390–420 nm region of time-resolved difference spectra in *A* and *B*. Conditions: 100 mM NaCl, 20 mM bis-Tris propane, pH 7.0, 16 μM bacteriorhodopsin.
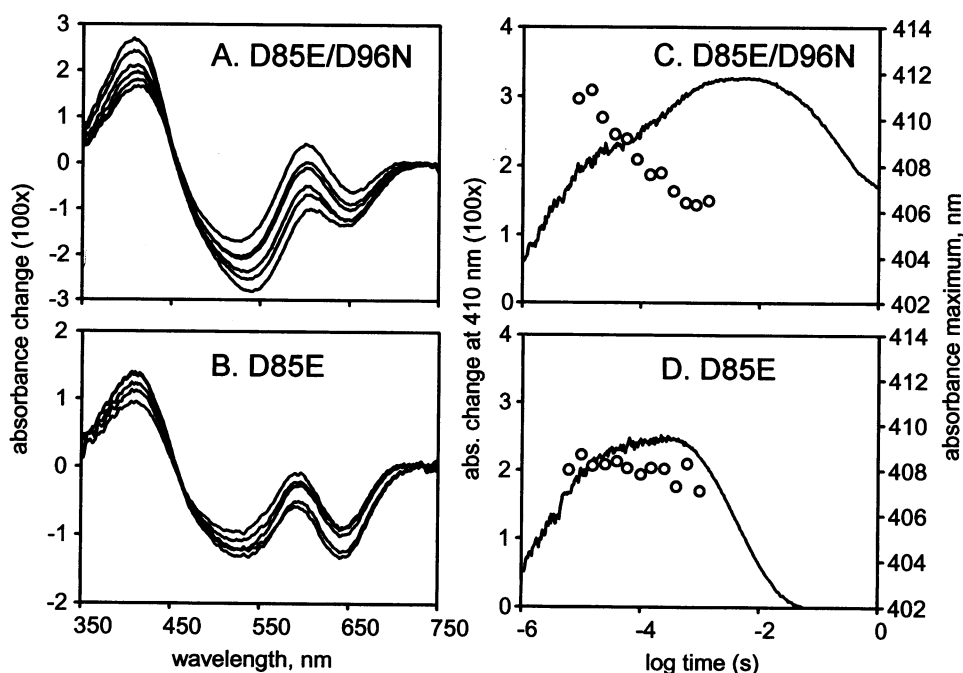
Table 1), and on the other hand locate the $M_1 \rightarrow M_2$ reaction near the third kinetic component of the formation of M (Figs. 8 and 9), much as reported in another study (Alexiev et al., 1994b).

However, the other results in this report (Figs. 4–7, and Tables 1 and 2) reinforce the conclusion (Heberle and Dencher, 1992; Heberle et al., 1993) that proton release is not directly linked to the Schiff base deprotonation. Because the two diverge under closer scrutiny, the temporal coincidence between them under some conditions must be fortuitous. How can this be reconciled with the pH dependence of proton release that implies a closer connection, as discussed above? One possibility is that a protein conformation change occurs between deprotonation of the Schiff base and the proton release, and decouples the two processes (Heberle and Dencher, 1992; Heberle et al., 1993). This would make, in effect, the M_1 to M_2 reaction a more complex one than was originally thought. A simpler explanation is suggested by modeling the consequences of various alternative schemes on the observable kinetics. A simple scheme would have K, L, and M_1 in equilibrium but proton release in parallel with the $M_1 \rightarrow M_2$ reaction. Thus, the $M_1^{(0)}$ to M_2^{-1} overall reaction (where the superscripts indicate the net protonation state of the protein, i.e., of the proton release group XH) is described by two branches. One branch is $M_1^{(0)} \rightarrow M_1^{-1} \rightarrow M_2^{-1}$, and the other is $M_1^{(0)} \rightarrow M_2^{(0)} \rightarrow M_2^{-1}$. Many sets of rate constants can be found for this scheme that produce M formation kinetics approximately described by three components. Yet according to these simulations, even though the proton release occurs during the transitions between M substates, its time constant and kinetic behavior do not need to correspond to any of the phenomenological formation components of M (not shown).

In the classical version of the alternating access hypothesis for ion pumps, the ion-binding site is connected to either one membrane side or the other, but never to both. If the proton release can occur at virtually any time in the bacteriorhodopsin photocycle after protonation of D85, as we report, the alternating access mechanism for this system (Kataoka et al., 1994) cannot be this simple. Fig. 11 A illustrates the simplest model in which access of the deprotonated Schiff base (SB) alternates between the two membrane sides. This model requires the temporal separation of proton release from proton uptake. Fig. 11 B shows a more complex model, in which D85 is permanently connected to the extracellular side and the internal transfer of the Schiff base proton to D85 results in a conformational shift (Kataoka et al., 1994) that splits the active site and connects the now unprotonated Schiff base to the cytoplasmic side. Its reprotonation is by a complex that includes D96 and other hydrogen-bonding residues, as well as bound water that regulates the pK_a of D96 (Cao et al., 1991; Brown et al., 1994b). In this model, the proton release and uptake are independent of one another, as was proposed earlier on the basis that their temporal sequence could be manipulated at will by introducing mutations that changed specific rate constants (Brown et al., 1994b). This model is consistent also with the results in the present study, because
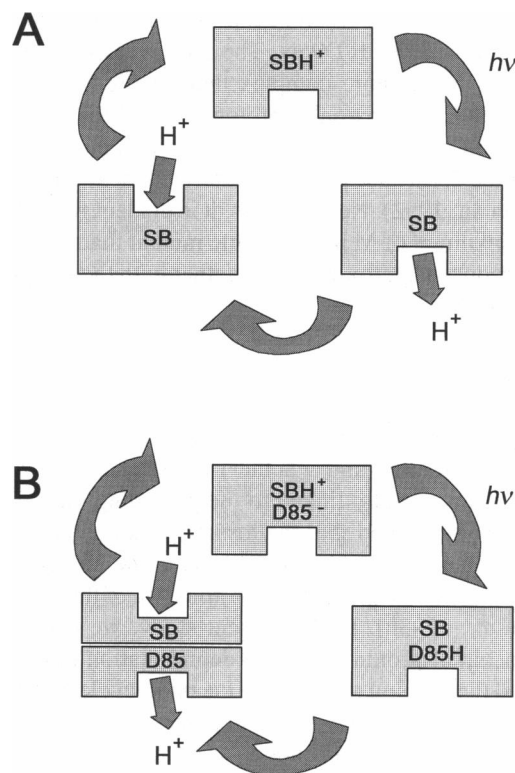

FIGURE 11 Two alternative versions of the alternative access hypothesis for proton transport by bacteriorhodopsin. (A) The connectivity of the Schiff base simply changes from one membrane surface to the other during the transport cycle. (B) The Schiff base is connected to the proton acceptor D85 in the unphotolyzed state, whereas D85 is connected to one of the membrane surfaces. After proton transfer to D85, the connection between the Schiff base and D85, but not the connection of D85 to the membrane surface, is broken, and a connection between the other membrane surface and the Schiff base is established. The two versions are distinguished by the fact that in A the active site is the Schiff base and its connectivity is either to one side or the other, but in B the active site includes also D85 and the essence of the mechanism is that the switch establishes individual connectivities for the Schiff base and D85.

whereas proton release must occur after protonation of D85, it need not correlate with chromophore reactions, such as the reprotonation of the Schiff base and the reprotonation switch.

In Fig. 11 the extracellular access is shown as open for the unphotolyzed protein as proposed previously (Kataoka et al., 1994), and because without photoexcitation the Schiff base remains protonated, this needs an explanation. Deprotonation of the Schiff base in unphotolyzed bacteriorhodopsin is thermodynamically disfavored. Nevertheless, its access is to the extracellular surface, because when the pK_a of the Schiff base is lowered upon replacing the retinal with an analog, deprotonation to the extracellular side will occur upon increasing the pH, even if slowly (Kataoka et al., 1994) because of the low proton affinity of D85.

REFERENCES

Alexiev, U., T. Marti, M. P. Heyn, H. G. Khorana, and P. Scherrer. 1994a. Surface charge of bacteriorhodopsin detected with covalently bound pH indicators at selected extracellular and cytoplasmic sites. *Biochemistry.* 33:298–306.

Alexiev, U., T. Marti, M. P. Heyn, H. G. Khorana, and P. Scherrer. 1994b. Covalently bound pH-indicator dyes at selected extracellular or cytoplasmic sites in bacteriorhodopsin. 2. Rotational orientation of helices D and E and kinetic correlation between M formation and proton release in bacteriorhodopsin. *Biochemistry.* 33:13693–13699.

Balashov, S. P., R. Govindjee, M. Kono, E. Imasheva, E. Lukashev, T. G. Ebrey, R. K. Crouch, D. R. Menick, and Y. Feng. 1993. Effect of the arginine-82 to alanine mutation in bacteriorhodopsin on dark adaptation, proton release, and the photochemical cycle. *Biochemistry.* 32:10331–10343.

Bousché, O., S. Sonar, M. P. Krebs, H. G. Khorana, and K. J. Rothschild. 1992. Time-resolved Fourier transform infrared spectroscopy of the bacteriorhodopsin mutant Tyr-185-Phe: Asp-96 reprotonates during O formation, Asp-85 and Asp-212 deprotonate during O decay. *Photochem. Photobiol.* 56:1085–1095.

Braiman, M. S., T. Mogi, T. Marti, L. J. Stern, H. G. Khorana, and K. J. Rothschild. 1988. Vibrational spectroscopy of bacteriorhodopsin mutants: light-driven proton transport involves protonation changes of aspartate residues 85, 96, and 212. *Biochemistry.* 27:8516–8520.

Brown, L. S., L. Bonet, R. Needleman, and J. K. Lanyi. 1993. Estimated acid dissociation constants of the Schiff base, asp-85 and arg-82 during the bacteriorhodopsin photocycle. *Biophys. J.* 65:124–130.

Brown, L. S., Y. Gat, M. Sheves, Y. Yamazaki, A. Maeda, R. Needleman, and J. K. Lanyi. 1994a. The retinal Schiff base-counterion complex of bacteriorhodopsin: changed geometry during the photocycle is a cause of proton transfer to aspartate 85. *Biochemistry.* 33:12001–12011.

Brown, L. S., Y. Yamazaki, M. Maeda, L. Sun, R. Needleman, and J. K. Lanyi. 1994b. The proton transfers in the cytoplasmic domain of bacteriorhodopsin are facilitated by a cluster of interacting residues. *J. Mol. Biol.* 239:401–414.

Cao, Y., L. S. Brown, R. Needleman, and J. K. Lanyi. 1993a. Relationship of proton uptake on the cytoplasmic surface and the reisomerization of the retinal in the bacteriorhodopsin photocycle: an attempt to understand the complex kinetics of the protons and the N and O intermediates. *Biochemistry.* 32:10239–10248.

Cao, Y., G. Váró, M. Chang, B. Ni, R. Needleman, and J. K. Lanyi. 1991. Water is required for proton transfer from aspartate 96 to the bacteriorhodopsin Schiff base. *Biochemistry.* 30:10972–10979.

Cao, Y., G. Váró, A. L. Klinger, D. M. Czajkowsky, M. S. Braiman, R. Needleman, and J. K. Lanyi. 1993b. Proton transfer from asp-96 to the bacteriorhodopsin Schiff base is caused by decrease of the pK_a of asp-96 which follows a protein backbone conformation change. *Biochemistry.* 32:1981–1990.

Carmeli, C., A. T. Quintanilha, and L. Packer. 1980. Surface charge changes in purple membranes and the photoreaction cycle of bacteriorhodopsin. *Proc. Natl. Acad. Sci. USA.* 77:4707–4711.

Chronister, E. L., T. C. Corcoran, L. Song, and M. A. El-Sayed. 1986. On the molecular mechanisms of the Schiff base deprotonation during the bacteriorhodopsin photocycle. *Proc. Natl. Acad. Sci. USA.* 83: 8580–8584.

Diller, R., and M. Stockburger. 1988. Kinetic resonance Raman studies reveal different conformational states of bacteriorhodopsin. *Biochemistry.* 27:7641–7651.

Duñach, M., M. Seigneuret, J.-L. Rigaud, and E. Padros. 1988. Influence of cations on the blue to purple transition of bacteriorhodopsin: comparison of Ca^{2+} and Hg^{2+} binding and their effect on the surface potential. *J. Biol. Chem.* 263:17378–17384.

Eisfeld, W., C. Pusch, R. Diller, R. Lohrmann, and M. Stockburger. 1993. Resonance Raman and optical transient studies on the light-induced proton pump of bacteriorhodopsin reveal parallel photocycles. *Biochemistry.* 32:7196–7215.

Grzeisek, S., and N. A. Dencher. 1986. Time-course and stoichiometry of light-induced proton release and uptake during the photocycle of bacteriorhodopsin. *FEBS Lett.* 208:337–342.

Hanamoto, J. H., P. Dupuis, and M. A. El-Sayed. 1984. On the protein (tyrosine)-chromophore (protonated Schiff base) coupling in bacteriorhodopsin. *Proc. Natl. Acad. Sci. USA.* 81:7083–7087.

Heberle, J., and N. A. Dencher. 1990. Bacteriorhodopsin in ice: accelerated proton transfer from the purple membrane surface. *FEBS Lett.* 277:277–280.

Heberle, J., and N. A. Dencher. 1992. Surface-bound optical probes monitor proton translocation and surface potential changes during the bacteriorhodopsin photocycle. *Proc. Natl. Acad. Sci. USA.* 89: 5996–6000.

Heberle, J., D. Oesterhelt, and N. A. Dencher. 1993. Decoupling of photo- and proton cycle in the Asp85→Glu mutant of bacteriorhodopsin. *EMBO J.* 12:3721–3727.

Humphrey, W., I. Logunov, K. Schulten, and M. Sheves. 1994. Molecular dynamics study of bacteriorhodopsin and artificial pigments. *Biochemistry.* 33:3668–3678.

Jardetzky, O. 1966. Simple allosteric model for membrane pumps. *Nature.* 211:969–970.

Jencks, W. P. 1980. The utilization of binding energy in coupled vectorial processes. *Adv. Enzymol.* 51:75–106.

Jonas, R., Y. Koutalos, and T. G. Ebrey. 1990. Purple membrane: surface charge density and the multiple effect of pH and cations. *Photochem. Photobiol.* 52:1163–1177.

Kataoka, M., H. Kamikubo, F. Tokunaga, L. S. Brown, Y. Yamazaki, A. Maeda, M. Sheves, R. Needleman, and J. K. Lanyi. 1994. Energy coupling in an ion pump: the reprotonation switch of bacteriorhodopsin. *J. Mol. Biol.* 243:621–638.

Keszthelyi, L., and P. Ormos. 1980. Electrical signals associated with the photocycle of bacteriorhodopsin. *FEBS Lett.* 109:189–193.

Keszthelyi, L., and P. Ormos. 1989. Protein electric response signals from dielectrically polarized systems. *J. Membr. Biol.* 109:193–200.

Koch, M. H. J., N. A. Dencher, D. Oesterhelt, H.-J. Plöhn, G. Rapp, and G. Büldt. 1991. Time-resolved x-ray diffraction study of structural changes associated with the photocycle of bacteriorhodopsin. *EMBO J.* 10:521–526.

Kono, M., S. Misra, and T. G. Ebrey. 1993. pH dependence of light-induced proton release by bacteriorhodopsin. *FEBS Lett.* 331:31–34.

Korenstein, R., W. V. Sherman, and S. R. Caplan. 1976. Kinetic isotope effects in the photochemical cycle of bacteriorhodopsin. *Biophys. Struct. Mech.* 2:267–276.

Lanyi, J. K. 1993. Proton translocation mechanism and energetics in the light-driven pump bacteriorhodopsin. *Biochim. Biophys. Acta.* 1183: 241–261.

Lanyi, J. K., J. Tittor, G. Váró, G. Krippahl, and D. Oesterhelt. 1992. Influence of the size and protonation state of acidic residue 85 on the absorption spectrum and photoreaction of the bacteriorhodopsin chromophore. *Biochim. Biophys. Acta.* 1099:102–110.

Liu, S. Y. 1990. Light-induced currents from oriented purple membrane. I. Correlation of the microsecond component (B2) with the L-M photocycle transition. *Biophys. J.* 57:943–950.

Liu, S. Y., R. Govindjee, and T. G. Ebrey. 1990. Light-induced currents from oriented purple membrane. II. Proton and cation contributions to the photocurrent. *Biophys. J.* 57:951–963.

Mathies, R. A., S. W. Lin, J. B. Ames, and W. T. Pollard. 1991. From femtoseconds to biology: mechanism of bacteriorhodopsin's light-driven proton pump. *Annu. Rev. Biophys. Biophys. Chem.* 20:491–518.

Miller, A., and D. Oesterhelt. 1990. Kinetic optimization of bacteriorhodopsin by aspartic acid 96 as an internal proton donor. *Biochim. Biophys. Acta.* 1020:57–64.

Nakasako, M., M. Kataoka, Y. Amemiya, and F. Tokunaga. 1991. Crystallographic characterization by x-ray diffraction of the M-intermediate from the photocycle of bacteriorhodopsin at room temperature. *FEBS Lett.* 292:73–75.

Oesterhelt, D., and W. Stoeckenius. 1974. Isolation of the cell membrane of *Halobacterium halobium* and its fractionation into red and purple membrane. *Methods Enzymol.* 31:667–678.

Oesterhelt, D., J. Tittor, and E. Bamberg. 1992. A unifying concept for ion translocation by retinal proteins. *J. Bioenerg. Biomembr.* 24:181–191.

Otto, H., T. Marti, M. Holz, T. Mogi, M. Lindau, H. G. Khorana, and M. P. Heyn. 1989. Aspartic acid-96 is the internal proton donor in the reprotonation of the Schiff base of bacteriorhodopsin. *Proc. Natl. Acad. Sci. USA.* 86:9228–9232.

Otto, H., T. Marti, M. Holz, T. Mogi, L. J. Stern, F. Engel, H. G. Khorana, and M. P. Heyn. 1990. Substitution of amino acids Asp-85, Asp-212, and Arg-82 in bacteriorhodopsin affects the proton release phase of the pump and the pK of the Schiff base. *Proc. Natl. Acad. Sci. USA.* 87:1018–1022.

Rothschild, K. J. 1992. FTIR difference spectroscopy of bacteriorhodopsin: toward a molecular model. *J. Bioenerg. Biomembr.* 24:147–167.

Sampogna, R. V., and B. Honig. 1994. Environmental effects on the protonation states of active site residues in bacteriorhodopsin. *Biophys. J.* 66:1341–1352.

Scherrer, P., U. Alexiev, H. Otto, M. P. Heyn, T. Marti, and H. G. Khorana. 1992. Proton movement and surface charge in bacteriorhodopsin detected by selectively attached pH-indicators. *In* Structures and Functions of Retinal Proteins. J. Rigaud, editor. John Libbey Eurotext Ltd., Montrouge. 205–211.

Souvignier, G., and K. Gerwert. 1992. Proton uptake mechanism of bacteriorhodopsin as determined by time-resolved stroboscopic FTIR spectroscopy. *Biophys. J.* 63:1393–1405.

Subramaniam, S., M. Gerstein, D. Oesterhelt, and R. Henderson. 1993. Electron diffraction analysis of structural changes in the photocycle of bacteriorhodopsin. *EMBO J.* 12:1–8.

Szundi, I., and W. Stoeckenius. 1989. Surface pH controls purple-to-blue transition of bacteriorhodopsin: a theoretical model of purple membrane surface. *Biophys. J.* 56:369–383.

Tanford, C. 1983. Mechanism of free energy coupling in active transport. *Annu. Rev. Biochem.* 52:379–409.

Thorgeirsson, T. E., S. J. Milder, L. J. W. Miercke, M. C. Betlach, R. F. Shand, R. M. Stroud, and D. S. Kliger. 1991. Effects of Asp-96→Asn, Asp-85→Asn, and Arg-82→Gln single-site substitutions on the photocycle of bacteriorhodopsin. *Biochemistry.* 30:9133–9142.

Váró, G., and J. K. Lanyi. 1990. Pathways of the rise and decay of the M photointermediate of bacteriorhodopsin. *Biochemistry.* 29:2241–2250.

Váró, G., and J. K. Lanyi. 1991a. Thermodynamics and energy coupling in the bacteriorhodopsin photocycle. *Biochemistry.* 30:5016–5022.

Váró, G., and J. K. Lanyi. 1991b. Kinetic and spectroscopic evidence for an irreversible step between deprotonation and reprotonation of the Schiff base in the bacteriorhodopsin photocycle. *Biochemistry.* 30:5008–5015.

Wikström, M., and K. Krab. 1979. Proton pumping cytochrome *c* oxidase. *Biochim. Biophys. Acta.* 549:177–222.

Zimányi, L., Y. Cao, M. Chang, B. Ni, R. Needleman, and J. K. Lanyi. 1992a. The two consecutive M substates in the photocycle of bacteriorhodopsin are affected specifically by the D85N and D96N residue replacements. *Photochem. Photobiol.* 56:1049–1055.

Zimányi, L., G. Váró, M. Chang, B. Ni, R. Needleman, and J. K. Lanyi. 1992b. Pathways of proton release in the bacteriorhodopsin photocycle. *Biochemistry.* 31:8535–8543.